Journal of Fluorescence, Vol. 12, Nos. 3/4, December 2002 (© 2002)

The Susceptibility of Non-UV Fluorescent Membrane Dyes to Dynamical Properties of Lipid Membranes

Steffen Härtel,[1–3] Svitlana Tykhonova,[1] Marcus Haas,[1] and Horst A. Diehl[1]

Received April 8, 2002; revised July 3, 2002; accepted July 6, 2002

Fluorescence spectroscopy and microscopy are powerful techniques to detect dynamic properties in artificial and natural lipid membrane systems. Unfortunately, most fluorescent dyes that sense dynamically relevant membrane parameters are UV sensitive. Their major disadvantage is a high susceptibility to fluorescence bleaching. Additionally, the risk for hazardous damages in biological components generally increases with decreasing excitation wavelength. Therefore the use of non-UV–sensitive membrane dyes would provide significant advantage, particularly for applications in fluorescence microscopy, which usually implies high local excitation intensities. We applied steady-state fluorescence spectroscopy techniques to several UV and non-UV membrane dyes to detect and compare dynamically relevant excitation and emission characteristics. Small unilamellar liposomes (composed of egg yolk phosphatidylcholine) served as a model system for biological membranes. The dynamic properties of the membranes were varied by two independent parameters: the intrinsic cholesterol content (0–50 mol%) and temperature (10–50°C). We tested four non-UV–sensitive membrane dyes: 9-diethylamino-5H-benzophenoxazine-5-one (Nile Red), 4-(dicyanovinyl)julolidine (DCVJ), *N*-(3-triethylammoniumpropyl)-4-(4-(dibutylamino)styryl) pyridinium dibromide (FM 4-64), and 1,1′-dioctadecyl-3,3,3′,3′-tetramethylindocarbocyanine perchlorate ($DiIC_{18}$). We also tested three derivatives of $DiIC_{18}$: $DiIC_{16}$ and $DiIC_{12}$ differ in acyl chain length and Fast-$DiIC_{18}$ provides double bonds between hydrocarbon atoms. The spectral results were compared to established fluorescence characteristics of four UV membrane dyes: the anisotropy of 1-6-phenyl-1,3,5,-hexatrien (DPH), two derivatives of DPH (TMA-DPH and COO^--DHP), and the generalized polarization of 6-dodecanoyl-2-dimethyl-aminonaphthalene (Laurdan). Our results indicate that the tested non-UV dyes do not reveal dynamically relevant membrane parameters in a direct manner. However, spectral characteristics make $DiIC_{18}$, Nile Red, and DCVJ promising probes for the microscopic detection of lateral lipid organization, an indirect indicator of membrane dynamics. In particular, $DiIC_{18}$ showed very selective shifts in the emission spectra at defined temperatures and cholesterol contents that have not been reported elsewhere.

KEY WORDS: Membrane sensitive fluorescent dyes; membrane fluidity; membrane organization; generalized polarization; $DiIC_N$; steady-state fluorescence spectroscopy.

INTRODUCTION

The current discussion concerning the structure of biological membranes extends the classic fluid-mosaic

[1] Institute of Experimental Physics (Biophysics), University of Bremen, Box 330440, D-28334 Bremen, Germany.
[2] Facultad de Ciencias Químicas, Departemento de Química Biológica, Pabellón Argentina, Universidad Nacional de Córdoba, Ciudad Universitaria. 5000 Córdoba, Argentina & Centro de Estudios Científicos (CECS), Arturo Prat 514, Valdivia, Chile.
[3] To whom correspondence should be addressed. Tel: (0054) 351 433 41 68. Fax: (0054) 351 433 40 74. e-mail: shaertel@physik.uni-bremen.de

1053-0509/02/1200-0465/0

model [1] by important aspects. Recent experiments revealed different types of transversal and lateral organization patterns in lipid bilayers that help explain the diversity of membrane-related functions. Among the various types of membrane patterns (also referred to as microdomains) are superlattices, formed by defined lipid arrangements [2]; cavaeolae, consisting mainly of self-associating caveolin proteins and cholesterol [3]; and lipid rafts, mainly formed by sphingomyelin, glycosphingolipids, and glycosylphosphatidylinositol-anchored proteins in the presence of cholesterol [4].

In membranes, the formation of microdomains is strongly coupled to distinct dynamic properties, subsumed by the terms membrane fluidity or membrane microviscosity. Membrane microviscosity is directly connected to diffusion-controlled processes in cellular membranes [5]. It is furthermore involved in the localization and activity of many membrane-connected proteins [e.g., 6,7]. Malfunctions of regulatory mechanisms that control homeoviscosity in cellular membranes are discussed as a crucial factor for proper cell function or even survival [8,9]. On the other hand, rapid and selective reorganization of the lipid composition in plasma membranes is an important signaling process in necrobiology [10,11].

Reliable detection of membrane dynamics is still a difficult task. Direct, locally resolved access to dynamic properties in rather simple lipid patterns of liposomal membranes has not been achieved until recently [12–14]. Despite many restrictions, fluorescence spectroscopy and microscopy are important tools to detect dynamically relevant membrane parameters. Presently, microscopic techniques such as confocal or 2-photon microscopy [17], fluorescence lifetime microscopy [18], and fluorescence correlation spectroscopy [19] offer new approaches to resolve spatial distributions of dynamic parameters in lipid systems. Microscopic techniques are of interest because they access fluidity parameters or hyperstructures in cells under rather natural conditions [20].

ABBREVIATIONS: a.u., Arbitrary units; *bis*-pyrene, 1,3-*bis*-[1-pyrenyl]propane; Ch, cholesterol; COO^--DPH, (4-((6-phenyl)-1,3,5,-hexatrienyl)benzoic acid); DCVJ, (4-(dicyanovinyl)julolidine); $DiIC_{18/16/12}$, (1,1′-di-octa/hexa/do-decyl-3-3,3′,3′-tetramethylindocarbocyanine perchlorate); Fast-$DiIC_{18}$, (1,1′-dilinoleyl-3,3,3′,3′-tetramethylindocarbocyanine perchlorate); DMF, dimethylformamide; DLPC, dilaurayl phosphatedylcholine; DMPC, dimyristoyl phosphatidylcholine; DPPC, dipalmitoyl phosphatidylcholine; DMSO, dimethyl sulfoxide; DPH, 1-6-phenyl-1,3,5-hexatrien; em, emission; EPC, egg yolk phosphatidylcholine; exc, excitation; FM 4-64, (*N*-(3-triethylammoniumpropyl)-4-(4-(dibutylamino)styryl) pyridinium dibromide); LSM, laser scanning microscopy; Nile Red, 9-diethylamino-5H-benzophenoxazine-5-one; PC, phosphatidylcholine; PL, phospholipid; SR, sensitivity ratio; SUV, small unilamellar vesicles; TMA-DPH, 1-(4-trimethylammoniumphenyl)-6-phenyl-1,3,5-hexatrien.

Most fluorescent membrane dyes with molecular properties yielding dynamically relevant information provide spectral characteristics in the UV region. For such dyes, the following concepts for the parameterization of membrane fluidity have been established: The diffusion-controlled intermolecular excimer formation of pyrene and its derivatives [15,16]; the intramolecular excimer formation of pyrene-labeled lipid acyl chains [21] or *bis*-pyrenes [22]; the concept of rotational diffusion or fluorescence anisotropy (often performed with 1-6-phenyl-1,3,5,-hexatrien (DPH) and DPH-derivatives; Fig. 1b, c, and d and Fig. 2) [23–25]; the emission or excitation sensitive generalized polarization (GP_{em} or GP_{exc}) of 6-dodecanoyl-2-dimethylaminonaphthalene (Laurdan, Fig. 1a) [26].

The major disadvantage of UV excitation is the induction of rapid fluorescence bleaching and the possible damage of biological components. Two-photon excitation helps to avoid some of these problems [17], but this technique is not widely used. Therefore the use of non-UV membrane dyes offers important advantages for microscopic measurements in living cell populations.

Our study concentrates on the spectral characteristics of several non-UV membrane dyes (see Fig. 1e–h). Changes in their steady-state excitation and emission spectra are compared to the fluorescence characteristics of established UV dyes. We used small, unilamellar vesicles (SUV) prepared from egg yolk phosphatidylcholine (EPC). These liposomes represent an adequate compromise between the complex structure of cellular membranes and more homogeneously composed liposomes. We varied the dynamic properties of EPC membranes by changing the liposomal cholesterol content (0–50 mol%) and temperature (10–50°C). It is important to bear in mind that both temperature and cholesterol modify the fluidity of lipid membranes, but they interact in different ways with lipid dynamics and the incorporated fluorophors [22,27]. As a result, an independent variation of the parameters contributes complementary information to the properties of the system.

MATERIALS AND METHODS

Liposome Preparation

Egg yolk phosphatidylcholine (EPC) (Lipoid KG, Ludwigshaven, Germany) or EPC with varying amounts of cholesterol (Sigma) (1:0, 3:1, 3:2, 1:1, 1:2, mol[EPC]/mol[Ch]) were dissolved in 5 ml dichlormethane-methanol (2:1) to a final concentration of 2 mg/ml. Liquid was removed in a vacuum rotary evaporator at 30°C until a

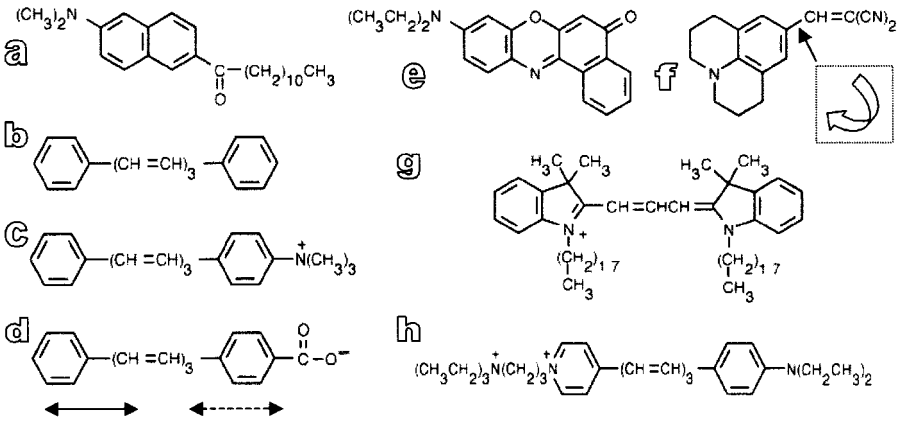

Fig. 1. Molecular structure of fluorescent membrane dyes. (a) Laurdan, (b) DPH, (c) TMA-DPH, (d) COO^--DPH, (e) Nile Red, (f) DCVJ, (g) $DiIC_{18}$, and (h) FM 4-64 (Modified structures from the Molecular Probes Catalogue). For DPH and its derivatives (b–d), the excitation and the emission dipole moments (↔) are nearly collinear to the main axis of the molecule [25]. The quantum yield, Φ_F, of the molecular rotor DCVJ is susceptible to the rotational freedom of the chemical bond outlined in (*f*) [31].

lipid film smoothly covered glass tube walls. After the extraction of the residual solvent by overnight storage in vacuum at 50°C, the lipid film was resuspended by vortexing in Tris buffer solution (100 mM Tris, pH 7.4). Small, unilamellar vesicles (SUV, with a medium diameter of 77.2 nm [28] were obtained by sonification for 15 min at 50°C (Sonopuls HD70, equipped with a titan-tip MS72, power = 70%, cycle = 30%, Bandelin), followed by ultracentrifugation (1 hr, 105,000 × *g*) to dispose non-incorporated components in the pellet. The final SUV lipid concentration was determined according to [29]. Liposome preparations were stored in darkness at 4°C and used within 2 weeks. Contact to oxidizing atmosphere was avoided by flushing with nitrogen. The quantification of the cholesterol to lipid content is described below.

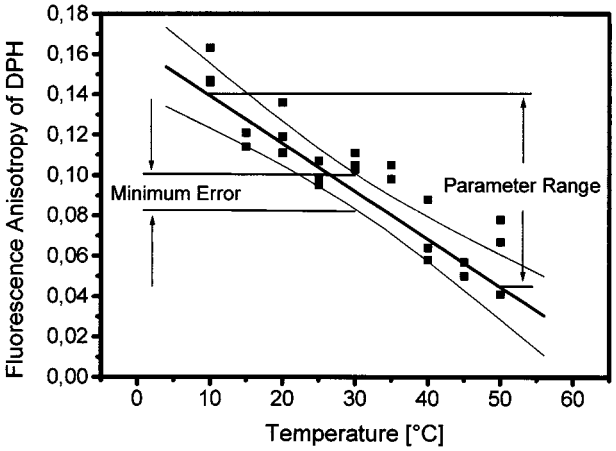

Fig. 2. Example of a linear regression analysis of DPH fluorescence anisotropy in small, unilamellar cholesterol-free EPC liposomes at different temperatures (10–50°C). The minimum distance between the 95% confidence bands (*black thin lines*) of the regression line (*black thick line*) defines the *minimum error.* The *parameter range* is defined by the distance between the maximum and the minimum fluorescence anisotropy signal of the regression line. The ratio of the parameter range and the minimum error defines the *sensitivity ratio* of the membrane dyes, which are plotted in Fig. 8. For all measurements, three samples of the liposome preparations were independently incubated with the corresponding membrane dyes.

Cholesterol Determination in SUV Liposomes

After lipid extraction of liposomes in chloroform/methanol [2:1], phospholipids and cholesterol were separated by thin layer chromatography. Phospholipids were exposed to 200°C for 4 hr, and the remaining phosphor was quantified calorimetically according to [30]. Quantification of cholesterol was achieved by gas chromatography (Perkin Elmer 840), using the following parameters: Column: 15 M × 250 μm × 0.1 μm DB-5cb (Seekamp, Germany). Temperature of injection: 275°C. Temperature of the flame ionisation detector: 275°C. Pressure of the carrier gas (He): 0.8 bar. Splitting ratio: 1:10. Temperature was set: 200°C isotherm for 3 min 200 to 275°C (6°C/min), and 275°C isotherm for 1.5 min. The final cholesterol content in the SUV preparations was: SUV group A: 0 mol% (100 × mol[Ch]/(mol[PL] + mol[Ch])), group B: 15 mol%, group C: 25 mol%, group D: 33 mol%, and group E: 50 mol%.

Fluidity Sensitive Fluorescent Membrane Dyes

All membrane dyes were purchased from Molecular Probes (MoBiTec, Göttingen, Germany). The UV-sensi-

tive membrane dyes DPH, 1-(4-trimethylammoniumphenyl)-6-phenyl-1,3,5,-hexatrien (TMA-DPH), 4-((6-phenyl)-1,3,5,-hexatrienyl)benzoic acid (COO^--DPH), and Laurdan were used as a reference for the spectral behaviour of seven non-UV sensitive membrane dyes.

Nile Red

The uncharged fluorophor Nile Red (Fig. 1e) is virtually non-fluorescent in aqueous environment. Spectral shifts in its emission and excitation spectra have been reported in different lipid environments [31,32].

DCVJ (4-(Dicyanovinyl)Julolidine)

DCVJ is a representative of a group of fluorophors frequently referred to as fluorescent molecular rotors. The quantum yield of torsional relaxing fluorophors Φ_F is susceptible to the intrinsic rotational freedom defined by the chemical bond that connects two intramolecular chromophores (see Fig. 1f) and to the restriction by the environmental free volume [34]. Φ_F can be connected to the viscosity η (or inverse fluidity) of the environment according to the Förster-Hoffmann expression [35]: $\log \Phi_F = C + \log \eta^{\chi}$. χ is defined by the intrinsic structural characteristics of the corresponding molecular rotor [36], and C is a constant. Φ_F increases with decreasing free volume, that is, an increase of the packing density of a bilayer. Kung and Reed [36] determined microviscosities in DPPC-bilayers and suggested the torsional relaxation of DCVJ to be directly dependent on the reorientation dynamics of the hydrocarbon chains within the center of membranes.

$DiIC_{18}$ (1,1′-Dioctadecyl-3,3,3′,3′-Tetramethylindocarbocyanine Perchlorate), $DiIC_{16}$, $DiIC_{12}$, Fast-$DiIC_{18}$

The non-toxic fluorophor $DiIC_{18}$ and its derivatives bind irreversibly and selectively to the outer membrane layer. A large polar fluorescent head group is attached to two acyl chains, which anchor well into the hydrocarbon chain region of membrane lipids (see Fig. 1g). The head group is supposed to be located slightly above the lipid head groups. Carbocyanine dyes are frequently used for the investigation of cellular fusion processes [37,38], for adhesion [39], and for migration [40]. They have also been used to derive fluidity-relevant information applying fluorescence recovery after photobleaching (FRAP) techniques [41,42] and fluorescence correlation spectroscopy [19]. $DiIC_{16}$ and $DiIC_{12}$ provide shorter acyl chain length than $DiIC_{18}$. Fast-$DiIC_{18}$ includes double bonds at the ninth and the twelfth carbon atom of each chain. The different properties of the acyl chains lead to a preferential incorporation into lipid matrices of similar characteristics [43], including selective partitioning into fluid or rigid lipid phases [44].

FM 4-64 (N-(3-Triethylammoniumpropyl)-4-(4-(Dibutylamino)Styryl) Pyridinium Dibromide)

Like $DiIC_N$, FM 4-64 (see Fig. 1h) attaches selectively to the outer membranes of lipid vesicles or cells, where its fluorescence intensity is strongly enhanced [45]. However, the binding is weak, implying a diffusion-controlled staining equilibrium among accessible membranes. Among the applications of FM 4-64 (and the more frequently used derivative FM 1-43) are visualizations of endo- and exozytotic processes [46,47] or cellular organelles [48]. Because no cytotoxic effects have been reported, the fluorophor is well suited for *in vivo* and *in vitro* investigation of cellular processes.

Dye-Incubation and Fluidity Measurements

Stock solutions of DPH, TMA-DPH, COO^--DPH, and Laurdan were prepared in dimethylformamide (Janssen, Geel, Belgium). Nile Red, $DiIC_{18/16/12}$, Fast-$DiIC_{18}$, FM 4-64, and DCVJ were dissolved in DMSO. Equivalents from stock solutions were added to 5 ml of SUV suspensions: 25 μg/ml PL in buffer for FM 4-64 and 10 μg/ml for all other dyes. DPH, TMA-DPH, and COO^--DPH were added to a final concentration of 160 nM. Laurdan: 12.8 nM. DCVJ, $DiIC_{18/16/12}$, and Fast- $DiIC_{18}$: 96 nM. Nile Red: 320 nM. FM 4-64: 3.2 μM. Light-protected incubation at room temperature was carried out for 1 hr. All measurements were carried out in quartz cuvettes of 1 cm^2 cross section with a Perkin Elmer LS50B spectrofluorometer. Temperature was controlled to ±0.1°C with a water-circulating bath. Bandpasses of the excitation and emission monochromators were 4.5 nm for Laurdan, DPH, TMA-DPH, and COO^--DPH; 5 nm for Nile Red, $DiIC_{18/16/12}$, Fast- $DiIC_{18}$, and DCVJ; and 10 nm for FM 4-64.

Fluorescence anisotropy for DPH, TMA-DPH, and COO^--DPH was calculated according to [23]:

$$r = \frac{I_{II} - G \cdot I_{\perp}}{I_{II} + 2 \cdot G \cdot I_{\perp}}$$

where r is the steady-state fluorescence anisotropy and I_{II} and $I_{\perp}$ are the fluorescence intensities at 425 nm parallel and perpendicular to the polarization of the excitation light at 358 nm. G is the grating factor.

Excitation and emission generalized polarization (GP_{exc} and GP_{em}) of Laurdan were calculated and interpreted according to [26]. Emission maxima were detected at 436 nm (hydrophobic dye environment: cholesterol rich liposomes at low temperatures) and at 478 nm (hydrophilic dye environment: EPC liposomes without additional cholesterol at high temperatures). In the excitation spectra, maxima were detected at 386 nm for the hydrophobic dye environment and at 356 nm for the hydrophilic dye environment. GP_{exc} and GP_{em} were derived from:

- $GP_{exc} = (I_{436} - I_{478})/(I_{436} + I_{478})$, where I_{436} and I_{478} are the emission intensities at 436 and 478 nm, using an excitation wavelength of 350 nm.
- $GP_{em} = (I_{386} - I_{356})/(I_{386} + I_{356})$, where I_{356} and I_{386} are the emission intensities at 490 nm, with an excitation wavelength at 356 and 386 nm, respectively.

Because the GP-formulas for Laurdan offer a convenient description for any fluorescent two-state system with two equilibrating excitation or emission maxima, we also defined an excitation GP for $DiIC_N$: $DiIC_N$-$GP_{exc} = (I_{586} - I_{567})/(I_{586} + I_{567})$, where I_{586} and I_{567} are the emission intensities at 586 and 567 nm, using an excitation wavelength of 550 nm.

Criteria for the Cholesterol- and Temperature-Dependent Spectral Sensitivity of the Fluorophors

The sensitivity of the membrane dyes to detect cholesterol and temperature-induced fluidity changes in EPC liposomes was characterized by the parameter *sensitivity ratio* (SR) [22]. SR was defined by the ratio of the *Parameter Range* and the *Minimum Error* of the 95% confidence bands. The *minimum error* was defined by linear regression analysis (see Fig. 2).

RESULTS

The steady-state fluorescence characteristics of UV and non-UV fluidity-sensitive membrane dyes were evaluated in EPC-SUV membranes at different temperatures (10–50°C) and cholesterol content (0–50 mol%).

Figure 3 shows representative emission spectra of Nile Red (a, b), DCVJ (c, d), FM 4-64 (e, f), and $DiIC_{18}$ (g, h) in small, unilamellar EPC liposomes. In Fig. 3b, d, f, and h, only the intrinsic cholesterol content varied, and in Fig. 3a, c, e, and g, only the temperature changed. With increasing temperature, the total emission intensities of Nile Red, DCVJ, FM 4-64, and of $DiIC_N$ generally decrease. The emission peaks of Nile Red, DCVJ, and FM 4-64 hardly show any shifts to different wavelength. The same observation holds for the excitation spectra. Only for $DiIC_{18}$, a pronounced change of the emission peak to shorter wavelength can be observed with increasing temperature (Fig. 3g), whereas the characteristics of the excitation spectra of $DiIC_{18}$ remain unchanged (Fig. 6).

With rising cholesterol concentration, the emission intensities of Nile Red, DCVJ, FM 4-64, and $DiIC_{18}$ successively increase (see Fig. 3b, d, f, and h). The emission peak for Nile Red (b) and DCVJ (d) are clearly shifted to a lower wavelength, whereas for FM 4-64 (f), only a marginal shift can be observed. For $DiIC_{18}$, increasing cholesterol concentration induces a sudden decrease of the emission peak to shorter wavelength (see Fig. 3h). The excitation spectra of Nile Red, DCVJ, FM 4-64, and $DiIC_{18}$ only show the expected variation in the total intensities, but no significant changes of any spectral characteristics (for $DiIC_{18}$ see Fig. 6, for Nile Red, DCVJ, and FM 4-64 see [49]).

Figure 4 directly compares the characteristic changes of the normalized emission spectra of $DiIC_{18}$ (b, d, f, h) with the spectral behavior of Laurdan (a, c, e, g). The emission peak of both fluorophores displays a pronounced shift to a shorter wavelength when the liposomal cholesterol concentration increases (a, b). For Laurdan, the ratio between the two maxima changes gradually with increasing lipid rigidity (a). For $DiIC_{18}$ instead, rising membrane cholesterol only marginally affects the spectral characteristics between 0 and 25 mol%, while major changes of the spectra occur between 25 and 33 mol% (b). With temperature increasing from 10 to 50°C, the maxima of the normalized emission spectra of Laurdan shifts to a longer wavelength (e), whereas for $DiIC_{18}$, the opposite behavior can be observed (f). Again, the emission spectra of Laurdan are subdued to rather gradual changes, whereas for $DiIC_{18}$, the major shift occurs when temperature rises from 25 to 35°C.

The differences between the spectra of Laurdan and $DiIC_{18}$ become evident when the GP_{exc} values of the two fluorescent dyes are compared (see Fig. 4c, d, g, h). Whereas for Laurdan, the GP_{exc}-values increase steadily with rising cholesterol concentrations (c) and decrease smoothly with increasing temperature (g), the GP_{exc}-values of $DiIC_{18}$ show a more complex behavior. Major increases of GP_{exc} values are observed between 25 and 33 mol% of cholesterol (d) and between 25 and 35°C (h). In contrast to Laurdan, cholesterol-induced changes of the GP_{exc} values of $DiIC_{18}$ depend on the temperature range. SUV, incubated at temperatures between 10 and

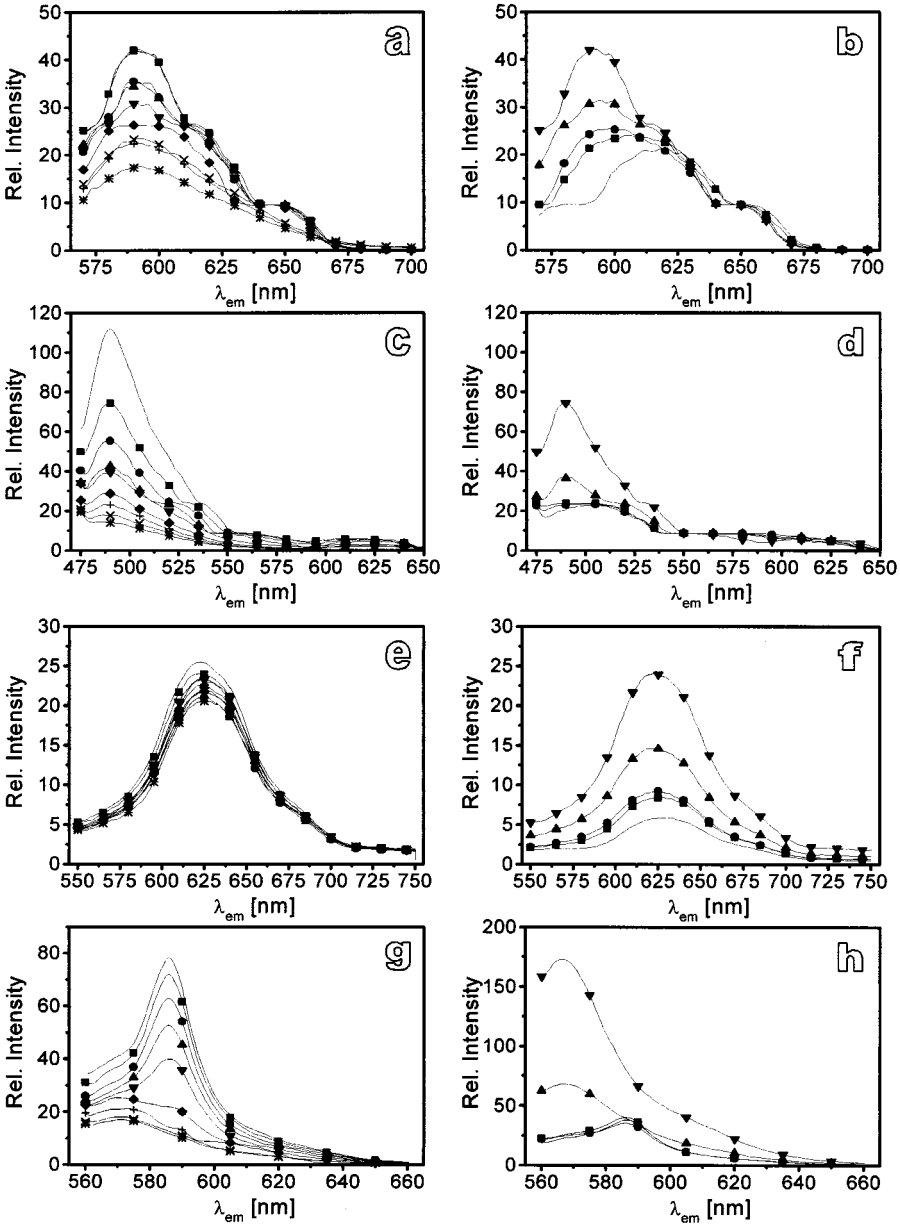

Fig. 3. Emission spectra of Nile Red (a, b: λ_{exc} = 470 nm), DCVJ (c, d: λ_{exc} = 465 nm), FM 4-64 (e, f: λ_{exc} = 573 nm), and $DiIC_{18}$ (g, h: λ_{exc} = 550 nm) in small, unilamellar EPC liposomes of different cholesterol content under the variation of temperature.
(a, c, e, g) Spectra at T = 10°C (−), 15°C (-■-), 20°C (-●-), 25°C (-▲-), 30°C (-▼-), 35°C (-♦-), 40°C (-+-), 45°C, (-×-), and 50°C (-*-).
(b, d, f, h) Spectra for cholesterol concentrations of 0 mol% (−), 15 mol% (-■-), 25 mol% (-●-), 33 mol% (-▲-), and 50 mol% (-▼-).
Spectra are shown for T = 15°C (b, d, f) and for T = 30°C (h). Cholesterol content was 50 mol% (a, c, e) and 15 mol% (h). Each spectra represents the mean of three independently stained liposomal preparations.

30°C are evidently affected to a higher degree than liposomes incubated between 40 and 50°C. Here, the GP_{exc} values of $DiIC_{18}$ posses a reduced sensitivity toward changes in the liposomal cholesterol content (d, h). The same observation holds for temperature-induced changes of the GP_{exc} values of $DiIC_{18}$ at constant cholesterol con-

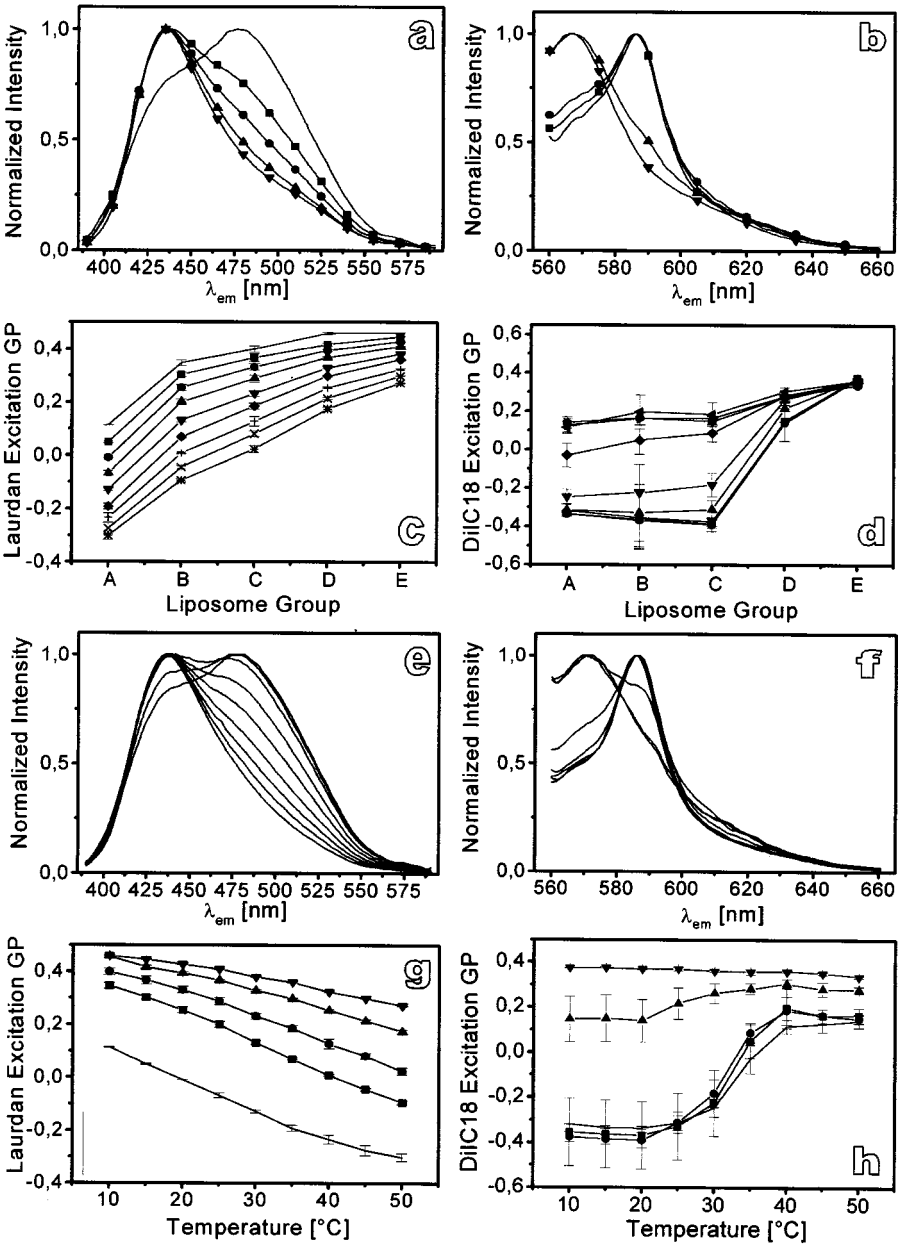

Fig. 4. Comparison of the emission characteristics of Laurdan and $DiIC_{18}$ in small, unilamellar EPC liposomes of different cholesterol content under the variation of temperature. (a, e) Normalized emission spectra of Laurdan (λ_{exc} = 350 nm). (b, f) Normalized emission spectra of $DiIC_{18}$ (λ_{exc} = 550 nm). (c, g) Excitation GP of Laurdan and $DiIC_{18}$ (d, h). (c, d) GP values are plotted for five cholesterol concentrations: Group A (0 mol%), B (15 mol%), C (25 mol%), D (33 mol%), and E (50 mol%). GP values were derived at T = 10°C (−), 15°C (-■-), 20°C (-●-), 25°C (-▲-), 30°C (-▼-), 35°C (-◆-), 40°C (-+-), 45°C, (-×-), and 50°C (-*-). (a, b, g, h). Different cholesterol concentrations are symbolized by (−): 0 mol%, (-■-): 15 mol%, (-●-): 25 mol%, (-▲-): 33 mol%, and (-▼-): 50 mol%. With increasing liposomal cholesterol concentration, the normalized emission maxima at higher wavelength disappears for Laurdan (a) and for $DiIC_{18}$ (b) (T = 30°C). With increasing temperature (10–50°C) instead, the normalized emission maxima at lower wavelength disappears for Laurdan (e), whereas for $DiIC_{18}$ (f), the normalized emission maxima at higher wavelength disappears again (cholesterol content = 15 mol%). Each spectra and GP value represents the mean of three measurements. Error bars were derived from standard deviation.

centrations. Whereas for Laurdan, temperature-induced changes of the GP_{exc} values affect all liposomal cholesterol concentrations virtually in the same manner (g), the GP_{exc} values of $DiIC_{18}$ in cholesterol-saturated liposomes (50 mol%) are completely insensitive toward temperature changes (d, h). At cholesterol concentrations of 33 mol%, a small temperature-dependent impact on the GP_{exc} values can be detected, whereas at cholesterol concentrations ranging from 25 to 0 mol%, the GP_{exc} values are equally susceptible to temperature changes (d, h). For Laurdan, the GP_{em} values derived from the excitation spectra support the results of the GP_{exc} values [49].

The influence of the acyl chain properties on the emission characteristics of the carbocyanine dyes tested can be followed by comparing the calculated GP values in Fig. 4d ($DiIC_{18}$) with Fig. 5a–c ($DiIC_{16}$, Fast-$DiIC_{18}$, and $DiIC_{12}$). The pronounced maximum at higher wavelength, observed under certain conditions with $DiIC_{18}$, diminishes successively from $DiIC_{16}$ to Fast-$DiIC_{18}$, and finally disappears for $DiIC_{12}$.

Figure 6 shows an example of the relative changes between the two excitation peaks in the excitation spectra of Laurdan. With increasing cholesterol content, the lower excitation peak decreases gradually. In contrast the normalized excitation spectra of $DiIC_{18}$ do not show temperature- or cholesterol-induced changes (Fig. 6). For $DiIC_{16}$, Fast-$DiIC_{18}$, and $DiIC_{12}$, the excitation spectra behave similar to that of $DiIC_{18}$ [49].

For Laurdan, $DiIC_{18}$, Nile Red, DCVJ, and FM 4-64, the most significant spectral changes induced by cholesterol and temperature in SUV are summarized in Fig. 7. The bivariate representations allow evaluation of the combined interactions of temperature and cholesterol content on the fluorescence parameters. Laurdan GP_{exc} values (Fig. 7a) decrease steadily from the rigid membrane environment to the fluid membrane environment. This continuous, steady behavior agrees well with the characteristics observed for other fluidity-sensitive parameters of UV-sensitive membrane dyes: the GP_{em} values of Laurdan; the anisotropy of DPH, TMA-DPH, and COO^--DPH; and the intermolecular excimer formation rate of pyrene or pyrene-methanol and the intramolecular excimer formation rate of *bis*-pyrene [22,27,49]. The maximum emission intensity values of Nile Red (c) and DCVJ (e) also support these characteristics, although the transition is not as smooth as observed with the UV dyes. For the maximum emission wavelength of Nile Red (d) and the maximum intensity of FM 4-64 (f), the transition of the fluorescence parameters are generally steeper for variations of the cholesterol content than for temperature-induced changes of the lipid environment. In Fig. 7b, the bivariate plot of the GP_{exc} values of $DiIC_{18}$

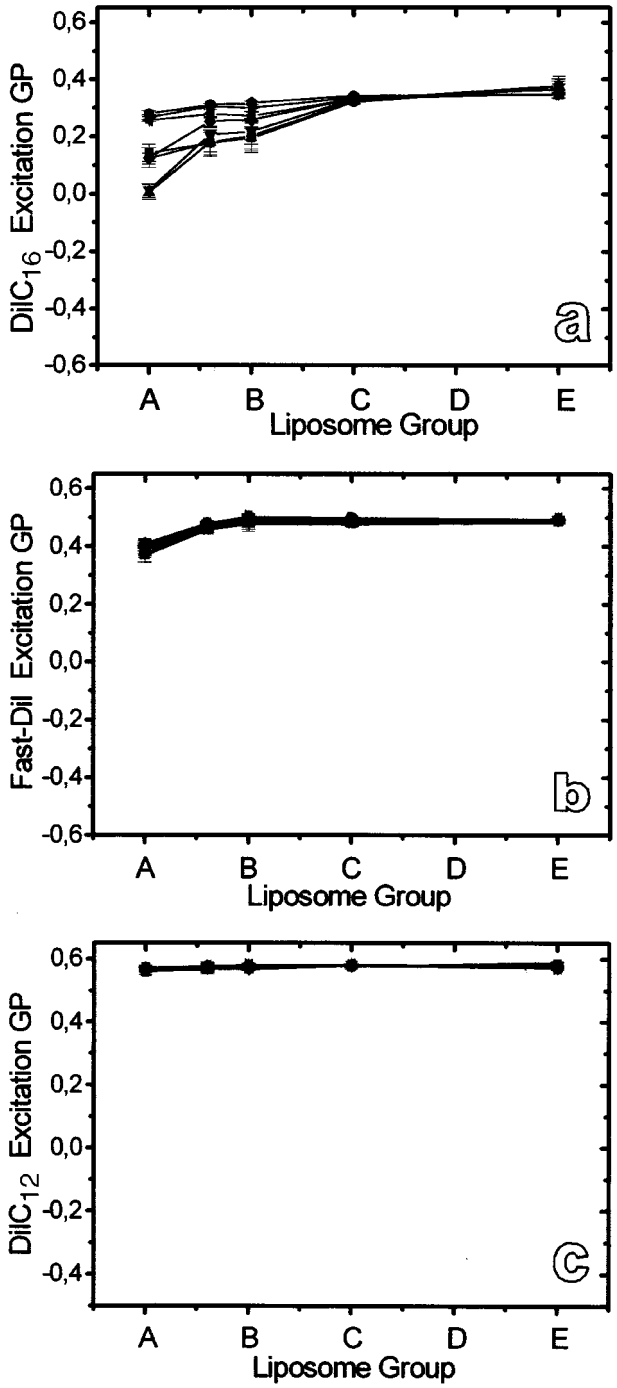

Fig. 5. GP values of $DiIC_{16}$ (a), Fast-$DiIC_{18}$ (b), and $DiIC_{12}$ (c) in small, unilamellar EPC liposomes of different cholesterol content under the variation of temperature. As in Fig. 4d, GP values are plotted for five cholesterol concentrations: Group A (0 mol%), B (15 mol%), C (25 mol%), D (33 mol%), and E (50 mol%). GP values were derived at T = 10°C (−), 15°C (-■-), 20°C (-●-), 25°C (-▲-), 30°C (-▼-), 35°C (-◆-), 40°C (-+-), 45°C, (-×-), and 50°C (-*-). GP values represent the mean of three measurements. Error bars were derived from standard deviation.

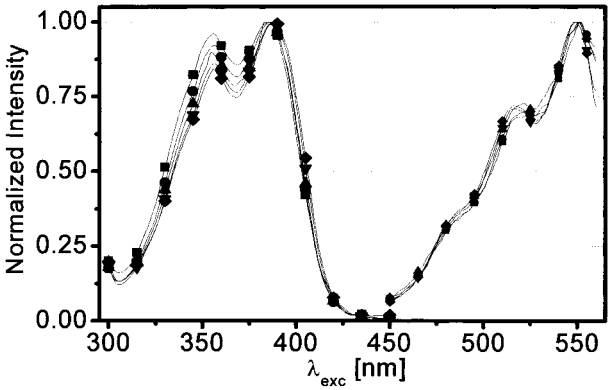

Fig. 6. Normalized excitation spectra of Laurdan (left, λ_{em} = 490 nm) and $DiIC_{18}$ (right, λ_{em} = 570 nm) in small, unilamellar EPC liposomes of different cholesterol content: 0 mol% (-■-), 15 mol% (-●-), 25 mol% (-▲-), 33 mol% (-▼-), and 50 mol% (-♦-). All measurements were performed at T = 15°C. Each spectra represents the mean of three independently stained liposomal preparations.

clearly visualizes the peculiar behavior of the fluorescence characteristics of this dye. A two-plateau system is formed with abrupt (phase-transition–like) changes of the GP_{exc} values.

The sensitivity ratio (SR), as defined in Fig. 2, displays the sensitivity of UV and of non-UV membrane dyes to detect cholesterol- and temperature-induced fluidity changes in EPC liposomes (Fig. 8a, b). For cholesterol-induced changes, the SR of the anisotropy of DPH outbalances the SR of the emission and the excitation GP of Laurdan, as well as the SR of the anisotropy of TMA-DPH and COO^--DPH. The parameters of the non-UV dyes are less sensitive toward cholesterol-induced changes (Fig. 8a). For temperature-induced variations of the lipid dynamics, both GP values of Laurdan are shown to be very sensitive parameters. Here, DPH, TMA-DPH, COO^--DPH, and the non-UV dyes show modest capacities (Fig. 8b). The calculation of the SR for the GP values of $DiIC_{18}$ has been omitted because of the non-linear behavior of this parameter (see Fig. 4d, h).

DISCUSSION

Dynamic properties of lipid membranes depend on external parameters such as pressure and temperature and on the intrinsic lipid composition, particularly on the fraction of cholesterol [27]. When fluorescent dyes are used to detect temperature-induced changes of membrane fluidity, it should be considered that the fluorescence characteristics of the probe are not only modulated by the lipid environment but also by the temperature itself. The same holds for cholesterol-induced changes. The risk of possible misinterpretation concerning these interactions can be minimized if temperature and cholesterol content are varied independently from each other.

Cholesterol-Induced Changes in Lipid Bilayers as Detected by Fluorescent Probes

Cholesterol is known to influence a variety of structurally and dynamically relevant parameters in a highly versatile way (for detailed discussion, see [26,50]). Across the membrane, cholesterol contributes sensitively to conformational, rotational, and translational dynamics of the acyl chains [51]. Laterally, cholesterol induces different phases in membranes of homogeneous lipid composition [26,52]. For microdomains such as cavaeolae and lipid rafts, a defined cholesterol concentration figures as an essential stabilizing factor [3,4,12]. Additionally, cholesterol is important for the formation of superlattices in biological membranes [2].

In heterogeneously composed liposomes, fluidity-dependent parameters of fluorescent membrane dyes such as DPH, TMA-DPH, pyrene, or *bis*-pyrene have indicated a steady rigidization with increasing cholesterol content [22]. The anisotropy values of DPH, TMA-DPH, and COO^--DPH, as well as the GP values of Laurdan and the shift in the emission maximum of Nile Red congruently indicate a steady change of the microviscosity (see Figs. 7 and 8). Whereas the amphiphile fluorophors TMA-DPH, COO^--DPH, and Laurdan are located near the head group region of lipid bilayers, the lipophilic membrane dyes DPH, Nile Red, pyrene, and *bis*-pyrene reliably report fluidity-sensitive fluorescence characteristics from the hydrophobic acyl chain region of the inner membrane. The observations indicate a steady rigidization throughout the depth of the EPC bilayers, with increasing cholesterol content in terms of the following characteristics:

(i) Less free volume for molecular rotation (DPH, TMA-DPH, and COO^--DPH, see Fig. 8a). Whereas the anisotropy values of DPH and its derivatives obtained in cholesterol-saturated SUV (50 mol%) resemble each other (∼0.3), the anisotropy values of DPH in cholesterol-free SUV (∼0.1) are clearly different from TMA-DPH (∼0.25), and COO^--DPH (∼0.18) [49]. The results indicate that the free rotational volume in the hydrophobic core of EPC bilayers is reduced to a higher degree than in the upper, more rigid acyl chain/glycerol region.

(ii) Less free volume for intramolecular conformational changes (*bis*-pyrene [22]) and for intramolecular rotation (DCVJ, see Fig. 3 d, Fig. 7 e, and Fig. 8 b).

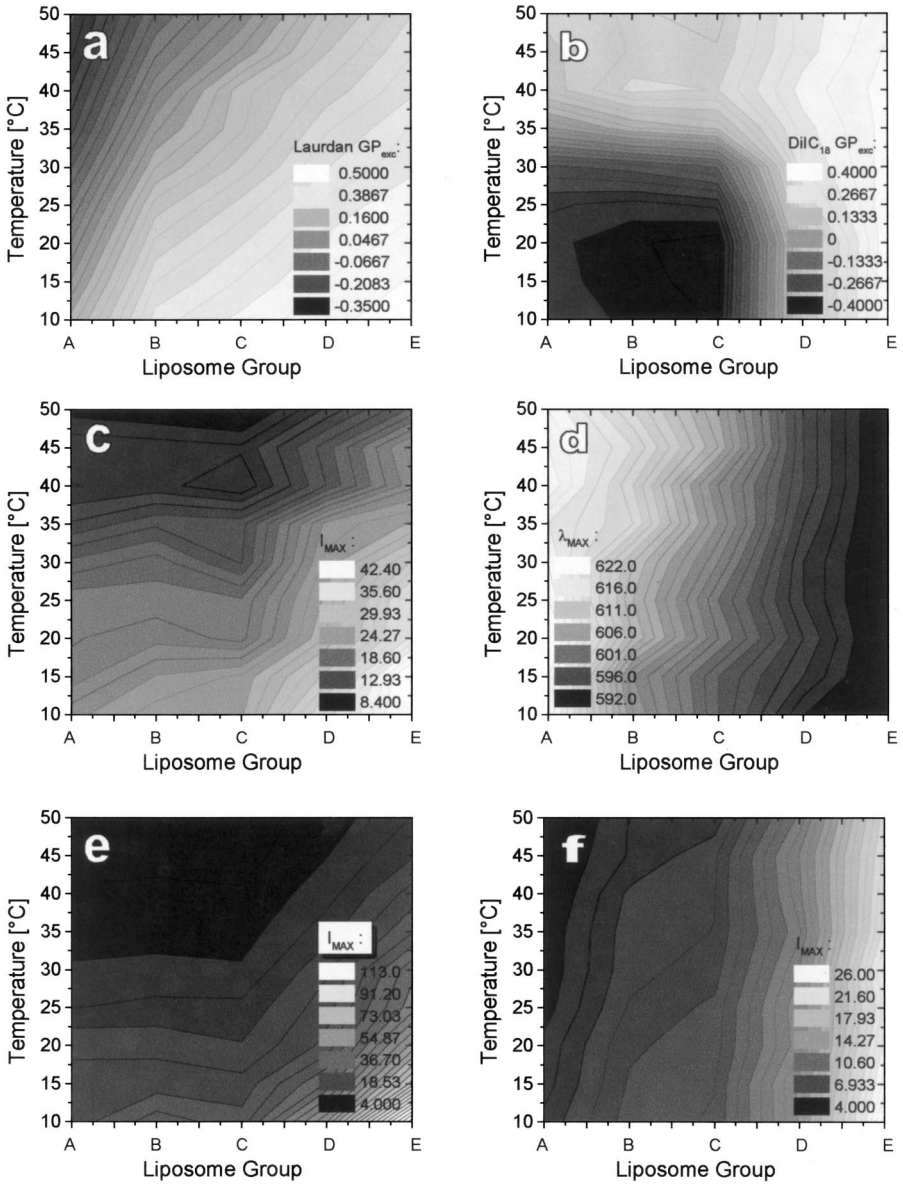

Fig. 7. Dynamically relevant parameters of fluorescent membrane dyes as a function of temperature (*y* axis, 10–50 °C) and cholesterol content (*x* axis, Liposome Group A: 0 mol%, B: 15 mol%, C: 25 mol%, D: 33 mol%, and E: 50 mol%). (a) Laurdan excitation GP. (b) $DiIC_{18}$ excitation GP. (c) Maximum emission fluorescence intensity of Nile Red [a.u.] (λ_{exc} = 470 nm). (d) Fluorescence emission maximum (λ_{max}) of Nile Red [nm] (λ_{exc} = 470 nm). (e) Maximum emission fluorescence intensity of DCVJ [a.u.] (λ_{exc} = 465 nm). (f) Maximum emission fluorescence intensity of FM 4-64 [a.u.] (λ_{exc} = 573 nm). Between the maximum and the minimum value of each parameter, 30 intermediate intervals are color-coded by gray values. Each value is derived from three independently stained liposomal preparations.

(iii) A closer packing of the bilayer, as indicated by a restricted diffusion (decreased excimer formation of pyrene) [22,27].

(iv) An inhibited penetration of water molecules into the membrane layer as detected by the increasing GP_{exc} values of Laurdan (see Fig. 4c). Solvent dipoles in the vicinity of Laurdan interact and align with the enhanced dipole moment of the dye in its excited state. Cholesterol attenuates water penetration into membranes, weakening the extent of dipolar relaxation processes [53].

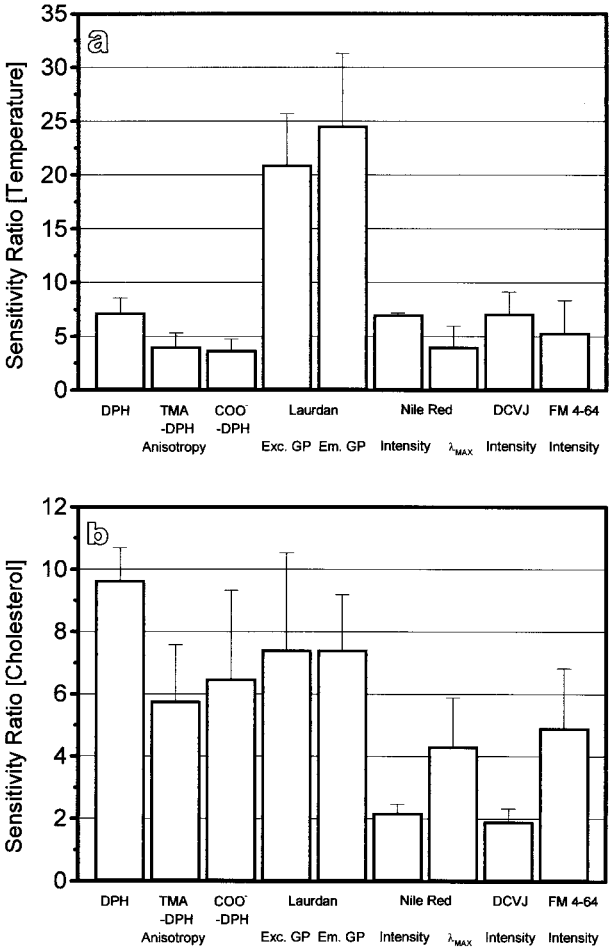

Fig. 8. Sensitivity ratios of fluidity-sensitive fluorescent membrane dyes as derived from measurements in small unilamellar EPC liposomes of (a) different cholesterol content (0–50 mol% and (b) under the variation of temperature (10–50°C).

(v) A decreased polarity or an enhanced order in the lipid arrangement of the polar head group area, as indicated by increasing GP_{em} values of Laurdan [54] and by the pronounced blue shift of the emission spectrum of Nile Red (see Fig. 3b).

In contrast to the gradual fluidity changes, the fluorescence characteristics of $DiIC_{18}$ show a discontinuous behavior when the cholesterol content rises from 25 to 33 mol% (see Fig. 4b and d). Possible reasons for this effects will be discussed below.

Temperature-Induced Changes as Detected by Fluorescent Probes

Like cholesterol, temperature can force the constituents of homogeneously composed lipid vesicles to adopt different lateral arrangements [26,52]. In EPC-SUV, DPH, TMA-DPH, COO^--DPH, and Laurdan indicate a steady decrease of the microviscosity with increasing temperature. The most significant changes were detected with DPH in the hydrophobic core region of the bilayers (see Fig. 8a) [49]. The emission intensity of DCVJ decreases with increasing temperature, indicating an increased intramolecular rotation of the molecule (see Fig. 3c, Fig. 7e, Fig. 8a) [36]. Accordingly, GP_{exc} and GP_{em} values of Laurdan sense an enhanced penetration of water molecules in the outer EPC-SUV membrane region. In contrast to the observation with cholesterol, the emission spectra of Nile Red do not express any changes besides a temperature-induced decrease of the total emission intensity (cf. Fig. 3a and b).

Concerning $DiIC_{18}$, increasing temperature provokes the same abrupt, peculiar changes in the emission characteristics as increasing cholesterol concentrations (see Fig. 3g, h; Fig. 4b, f). Again, the behavior of the other membrane dyes rather exclude that temperature-induced rearrangements of lipids are responsible for this effect.

In general, the behavior of the fluidity-sensitive parameters of the UV-sensitive membrane dyes reflects the expected dynamic conditions inside of heterogeneously composed membranes [22,27,54]. In contrast, the behavior of some non–UV-sensitive membrane dyes differs from what could be expected. It will therefore be discussed in detail below.

The Spectral Behavior of Nile Red

In a lipophilic environment, the fluorescent lifetime of Nile Red is prolonged and the quantum yield rises to almost 0.8 [55]. The excitation and emission spectra have been reported to shift to shorter wavelength with decreasing polarity [28,29,56,57,61]. This shift has originally been assumed to result from twisted intramolecular charge transfer (TICT) processes between the electron donor (diethylamine) and acceptor (condensed aromatic ring) groups of the dye [58] (see Fig. 1e). However, recent theoretical studies contradict the TICT model and support the hypothesis that increased dipole moments of the first excited molecular states cause this effect [55].

In EPC-SUV, the total emission intensity decreases with increasing temperature (see Fig. 1a) and with decreasing cholesterol content (see Fig. 1b). The emission spectra express a pronounced blue shift with increasing cholesterol content, but no such changes were detected with temperature. Additionally, the excitation spectra do not show any changes besides the variations of the total emission intensity [49]. In size and weight, Nile Red is

comparable to Laurdan. Because of a slightly positive charge of 0.015 (calculated for the nitrogen atom of the diethylamine group [59]), the dye should preferentially incorporate parallel to the acyl chains near the head group region of the lipids [60]. If, in analogy to Laurdan, the number of water molecules in the upper bilayer region provided a potential of interaction for Nile Red, the induced changes should result equally strong for cholesterol and temperature. Because the spectral shift of the emission peak exclusively occurs with changing amounts of cholesterol, an interpretation related to interactions with dynamic membrane, properties must be doubted. However, our results strongly support direct interactions of Nile Red with cholesterol. Because cholesterol-induced spectral shifts exclusively concern the emission spectra of Nile Red, the underlying interactions between the molecules are very likely to take place during the excited state of the dye.

The Spectral Behavior of DCVJ

The intensity variations of DCVJ, observed in EPC liposomes (see Fig. 3c, d), are in line with the interpretation of Kung and Reed [36]. The total emission intensity of DCVJ increases with membrane microviscosity. But in EPC vesicles the integral intensity changes should not be connected directly to torsional relaxation processes without the following severe reservation. Because temperature and cholesterol content both influence not only the distinct dynamic properties of membrane lipids but also the number of penetrating water molecules, the hydrophobic conditions, at least in the upper region of membranes, are subject to significant changes. Although the quantum yield of DCVJ has been reported to be independent from solvent polarity [36], the penetrating water alters the partition coefficient between a membrane and the embedding buffer. As a result, the total amount of fluorescent dyes inside of the membrane is reduced, and the total fluorescence emission intensity of the sample decreases (dilution effect). The magnitude of this effect can be estimated by observing the behavior of membrane dyes, which are insensitive to changes of free molecular volumes. We find the sensitivity ratio of the intensity variations of DCVJ to resemble the sensitivity ratios of the intensity spectra of Nile Red and FM 4-64 (see Fig. 8). Therefore, intensity variations induced by the changing partition coefficient seem to dominate the intensity variations resulting from changes of the free rotational volume. As a consequence, the total emission intensity of DCVJ cannot be regarded as a reliable parameter for microviscosity in liposomal membranes. In natural membranes, lateral membrane heterogeneities (e.g., rafts, cavaeolae, superlattices) are very likely to induce partition of hydrophobic probes. In this case, lateral intensity fluctuations of DCVJ cannot be associated unequivocally to microviscosity-induced changes of the quantum yield, Φ_F, or to concentration-dependent effects.

Apart from the intensity fluctuations of DCVJ, ref. [36] also reports a linear shift of the emission peak to longer wavelength with increasing dielectric constants. We confirm this effect in EPC liposomes with decreasing cholesterol content, but not with temperature (see Fig. 3c, d). This shift offers an approach to derive dielectric constants in cellular membranes by fluorescence microscopy, utilizing local derivations of the fluorescence intensities in various band pass channels.

The Spectral Behavior of FM 4-64

Voltage-dependent spectral shifts, spectral broadening, and changes on the quantum yield have been reported for styryl dyes in membranes [62]. The supplier (Molecular Probes) of the frequently used non-toxic styryl dye FM 1-43 reports the emission and absorption spectra to be subject to significant shifts dependent on the membrane environment. Our results clearly indicate that neither the emission nor the excitation spectra of the FM 1-43 derivative FM 4-64 (see Fig. 1h) show any substantial temperature- or cholesterol-induced shifts in EPC-SUV (see Fig. 3e, f). As a consequence, the spectra of FM 4-64 cannot reveal valuable information regarding lipid dynamics on a molecular level. Nevertheless, the generally favorable characteristics have made FM dyes valuable for the visualization of membrane dynamics on larger scales [46].

The Spectral Behavior of $DiIC_{18}$, $DiIC_{16}$, $DiIC_{12}$, and Fast-$DiIC_{18}$

Out of the non-UV sensitive membrane dyes, the amphiphilic fluorophore $DiIC_{18}$ (see Fig. 1g) shows the most particular spectral responses (see Fig. 3g, h). It becomes evident from the normalized emission spectra that the emission maxima is not subdued to steady shifts, but rather characterises a two-state emissive system, just as it is observed for the spectra of the UV-sensitive dye Laurdan (see Fig. 4a, b, e, f). But, whereas the generalized polarization of Laurdan responds rather gradually to changing temperature or cholesterol content (see Fig. 4c, d and Fig. 7a), the GP values derived for $DiIC_{18}$ approximately define a two-plateau system (see Fig. 4d, h and Fig. 7b). At high temperatures, cholesterol variations induce only small changes in the GP values, and high cholesterol concentrations prevent temperature-induced changes completely. These sudden transitions of the GP

value between 25 and 33 mol% of cholesterol and at temperatures between 25 and 35°C are not in line with the microviscosity-dependent fluorescent parameters of all other dyes (see Fig. 7 [22,27]). As a consequence, the course of the transition is not consistent with an interpretation based on microviscous changes (compare Fig. 7a and b).

EPC contains approximately 30% C_{16}, 60% C_{18}, and 10% lipids with longer, unsaturated hydrocarbon chains. The longer wavelength emission peak successively diminishes, following $DiIC_{18} \gg DiIC_{16} > \text{Fast-}DiIC_{18} > DiIC_{12}$ (see Fig. 4d and Fig. 5). Because the strength of the incorporation of the diacylcarbocyanine dyes into lipid bilayers is primarily defined by the matching of the acyl chain characteristics of the components, the generation of the observed emission peak and the binding affinity of $DiIC_N$ are strongly related. The question induced by our data concerns the distinguished membrane parameters that provide the environmental conditions at cholesterol concentrations below 25 mol% and temperatures below 25°C. An explication may be provided by one of the following hypotheses:

(i) Dimers or higher-ordered $DiIC_{18}$ aggregates may be formed under certain membrane conditions.
(ii) A temperature- or cholesterol-induced relocation of the fluorescent head group of $DiIC_{18}$-molecules, either deeper into or farther off the lipid matrix. As a consequence, the polarity of the environment could alter the fluorescence emission.
(iii) Intermolecular coupling between single membrane constituents and the dye.

$DiIC_{18}$ is a representative of a large family of cyanine dyes that incorporate into lipid bilayers and interact noncovalently with various membrane constituents and distinct membrane properties. Since the 1970s, cyanine dyes have been extensively studied to monitor membrane potentials in living cells (e.g., [62]). The probes provide clear partition preferences for coexisting gel and fluid phases that depend on the matching of the length and the degree of saturation between the acyl chains of the bilayer lipids and the acyl chains attached to the dye. Lipid/dye partitioning was evaluated in model systems [43,44,64], as well as in living cells [65]. Absorption and emission dipoles of $DiIC_{18}$ form an angle of ~20°, facilitating the application of spectrometric or microscopic anisotropy concepts in cells [66,67]. Membrane lipid flow has been determined in leukocytes by measuring fluorescence recovery after photobleaching of $DiIC_{16}$ [68], and single molecule fluorescence techniques have been performed with fluorescence correlation spectroscopy [19].

Despite the intensive use of the dyes, we found no hint to explain the emission peak observed at 586 nm. Packard and Wolf [69] reported average fluorescence lifetimes to be dependent upon lipid phases and to a smaller degree, upon surface charges and phospholipid head groups. They also found the fluorescence lifetime of $DiIC_{18}$ to be sensitive to cholesterol and thus membrane organization, detecting an extended fluorescence lifetime in DPPC/cholesterol liposomes at cholesterol concentrations between 10 and 45 mol%. Sims *et al.* [63] mention the formation of dimers and larger-size $DiIC_{18}$ aggregates with consequences on spectral characteristics and quantum yields in red blood cell membranes. Packard and Wolf [69] supported this thesis by reporting a marked decay in fluorescence lifetime, when $DiIC_{18}$ concentrations exceeded 10^{-3} mol% in EPC membranes.

All fluorescence characteristics reported are rather inconsistent with hypothesis (ii). There are indications that the emission peak is red shifted about 20 nm when the dye incorporates from an aqueous environment into lipid membranes (DiS-C3(5) [63], and increasing membrane potential induces red shifts of about 10 nm (DiS-C3(3) [70]). But the observation that the lifetime of $DiIC_{18}$ is independent from the polarity of lipid head groups [63] contradicts hypothesis (ii). In our laboratory, water, DMF, ethanol, or cyclohexane do not alter the $DiIC_{18}$ emission spectra significantly (data not shown). Elongated fluorescence lifetime at intermediate cholesterol concentrations in DPPC vesicles [63] could support hypothesis (i) or (iii). Unfortunately the authors did not comment on possible wavelength shifts. In EPC liposomes, distinguished intermolecular lipid–dye interactions or $DiIC_{18}$ aggregates could very well be inhibited above a defined cholesterol concentration or temperature (see Fig. 4).

No experiment to date rejects hypothesis (i) or (iii). Experiments in model systems that couple lifetime spectra and anisotropy data will certainly reveal the answer to this question in the future. Because excitation spectra of $DiIC_{18}$ lack any notable perturbation, the spectrometrically relevant interactions must occur during the lifetime of the excited state of the molecule (see Fig. 6).

CONCLUSION

Although the non-UV membrane dyes presented in this paper do not reveal dynamically relevant membrane parameters in a direct manner, the spectral changes in the emission characteristics of $DiIC_{18}$, Nile Red, and DCVJ in dependence of the cholesterol content make these dyes

promising tools for the microscopic detection of heterogeneous membrane compartments in living cells. Because defined lipid environments correlate with dynamic properties of biological membranes, the emission properties of the dyes allow local estimations of membrane fluidities in an indirect manner.

ACKNOWLEDGMENTS

We thank Mrs. Edda Toma and Mrs. Christina Kernst for the work in the laboratory. We are grateful to Dr. Maria Engelke and Dr. Bruno Maggio for constructive discussions on the manuscript, and to Mrs. Andrea Ciminari for carefully reading the English version. S. H. is a Feodor-Lynen-Fellow of the Alexander v. Humboldt Foundation and a Postdoctoral Fellow of CONICET.

REFERENCES

1. S. A. Singer and G. L. Nicolson (1972) The fluid mosaic model of the structure of the cell membranes. *Science* **173**, 720–731.
2. P. Somerharju, J. A. Virtanen, and H. K. Cheng (1999) Lateral organization of membrane lipids. The superlattice view. *Biochim. Biophys. Acta* **1440**(1), 32–48.
3. R. G. Parton (1996) Caveolac and caveolins. *Curr. Opin. Cell Biol.* **8**, 542–548.
4. K. Simons and E. Ikonen (1997) Functional rafts in cell membranes. *Nature* **387**, 569–572.
5. H. Kutchai, R. A. Cooper, and R. E. Forster (1980) Effect of anesthetic alc. and alt. in the level of membrane cholesterol in erythrocyte water permeability. *Biochim. Biophys. Acta* **600**, 542–552.
6. L. P. Zanello, E. Aztiria, S. Antollini, and F. J. Barrantes (1996) Nicotinic acetylcholine receptor channels are influenced by the physical state of their membrane environment. *Biophys. J.* **70**, 2155–2164.
7. S. S. Antollini, M. A. Soto, I. Bonini de Romanelli, C. Gutierrez-Merino, P. Sotomayor, and F. J. Barrantes (1996) Physical state of bulk and protein-associated lipid in nicotinic acetylcholine receptor-rich membrane studied by Laurdan generalized polarization and fluorescence energy transfer. *Biophys. J.* **70**, 1275–1284.
8. F. Ojeda, H. A. Diehl, and H. Folch (1994) Radiation-induced membrane changes and programmed cell death: possible interrelationships. *Scan. Microscopy* **8**, 645–651.
9. S. Härtel, F. Ojeda, and H. A. Diehl (1998) Cholesterol induced variations of membrane dynamics related to the induction of apoptosis in mouse thymocytes. *Int. J. Radiat. Biol.* **74**, 607–615.
10. V. A. Fadok, D. R. Voelker, P. A. Campbell, J. J. Cohen, D. L. Bratton, and P. M. Henson (1992) Exposure of phosphatidylserine on the surface of apoptotic lymphocytes triggers specific recognition and removal by macrophages. *J. Immunol.* **148**, 2207–2216.
11. Z. Darzynkiewicz, G. Juan, X. Li, W. Gorczyca, T. Murakami, and F. Traganos (1997) Cytometry in cell necrobiology: analysis of apoptosis and accidental cell death (necrosis). *Cytometry* **27**, 1–20.
12. C. Dietrich, L. A. Bagatolli, Z. N. Volovyk, N. L. Thompson, M. Levi, K. Jacobson, and E. Gratton (2001) Lipid Rafts Reconstituted in Model Membranes. *Biophys. J.* **80**, 1417–1428.
13. L. A. Bagatolli and E. Gratton (1999) Two photon fluorescence microscopy observation of shape changes at the phase transition in phospholipid's giant unilamellar vesicles. *Biophys. J.* **77**, 2090–2101.
14. L. A. Bagatolli and E. Gratton (1999) Two-photon fluorescence microscopy of coexisting lipid domains in giant unilamellar vesicles of binary phospholipid mixtures. *Biophys. J.* **78**, 290–305.
15. M. Engelke, T. Behmann, F. Ojeda, and H. A. Diehl (1994) Heterogeneity of microsomal membrane fluidity: evaluation using intrinsic tryptophan energy transfer to pyrene probes. *Chem. Phys. Lipids* **24**, 35–40.
16. M. Engelke, H. C. Klockmann, and H. A. Diehl (1995) Gramieidin effects on the transverse and lateral distribution of pyrene and pyrene derived probes in lipid bilayers. *Spectrochim. Acta* **51**, 1939–1947.
17. W. Yu, P. T. So, T. French, and E. Gratton (1996) Fluorescence generalized polarization of cell membranes: a two-photon scanning microscopy approach. *Biophys. J.* **70**, 626–636.
18. I. G. Krishnamoorthy (1998) Probing the dynamics of planar supported membranes by Nile red fluorescence lifetime distribution. *Biochim. Biophys. Acta* **1414**, 255–259.
19. P. Schwille, J. Korlach, and W. W. Webb (1999) Fluorescence correlation spectroscopy with single molecule sensitivity on cell and model membranes. *Cytometry* **1**, 176–182.
20. R. Varma and S. Mayor (1998) GPI anchored proteins are organised in submicron domains at the cell surface. *Nature* **394**, 798–801.
21. K. H. Cheng, S. Y. Chen, P. Butko, B. W. Van der Meer, and P. Somerharju (1991) Somerharju, Intramolecular excimer formation of pyrene-labeled lipids in lamellar and inverted hexagonal phases of lipid mixtures containing unsaturated phosphatidylethanolamine. *Biophys. Chem.* **39**, 137–144.
22. S. Härtel, H. A. Diehl, and F. Ojeda (1998) Methyl beta cyclodextrins and liposomes as water-soluble carriers for cholesterol incorporation into membranes and its evaluation by a microenzymatic fluorescence assay and membrane fluidity-sensitive dyes. *Anal. Biochem.* **258**, 277–284.
23. J. R. Lakowicz (1983) *Principles of Fluorescence Spectroscopy,* Plenum Press, New York.
24. J. G. Kuhry, P. Fonteneau, G. Duportail, C. Maechling, and G. Laustriat (1983) TMA-DPH: a suitable fluorescence polarization probe for specific plasma membrane fluidity studies in intact living cells. *Cell Biophys.* **5**, 129–140.
25. B. R. Lenz (1989) Membrane fluidity as detected by DPH probes. *Chem. Physics Lipids* **50**, 171–190.
26. T. Parasassi, A. M. Giusti, M. Raimondi, and E. Gratton (1995) Abrupt modifications of phospholipid bilayer properties at critical cholesterol concentrations. *Biophys. J.* **68**, 1895–1902.
27. A. G. Macdonald, K. W. J. Wahle, A. R. Cossins, and M. K. Behan (1988) Temperature, pressure and cholesterol effects on bilayer fluidity, a comparison of pyrene excimer/monomer ratios with the steady-state fluorescence polarization of diphenylhexatriene in liposomes and microsomes. *Biochim. Biophys. Acta* **938**, 231–242.
28. H. C. Klockmann (1993) *Untersuchungen zum Einfluβ von Intermolekularen Wechselwirkungen auf die Eignung von pyrenen als Sonden zur Messung der lateralen Diffusion in biologischen Membranen*. Ph.D. Thesis, University of Bremen, Bremen.
29. J. C. Stewart (1980) Colorimetric determination of phospholipids with ammonium ferrothiocyanate. *Anal. Biochem.* **104**, 10–14.
30. V. E. Vaskovsky and E. Y. Kostetsky (1968) Modified spray for the detection of phospholipids on thin-layer chromatograms. *J. Lipid Res.* **9**, 396.
31. J. F. Deye, T. A. Berger, and A. G. Anderson (1990) Nile red as a solvatochromic dye for measuring solvent strength in normal liquids and mixtures of normal liquids with supercritical and near critical fluids. *Anal. Chem.* **62**, 615.
32. D. L. Sackett and J. Wolff (1987) Nile Red As a polarity-sensitive fluorescent probe of hydrophobic protein. *Anal. Biochem.* **167**, 228–234.
33. C. E. Kung and J. K. Reed (1989) Fluorescent molecular rotors: a new class of probes for tubulin structure and assembly. *Biochemistry* **28**, 6678–6686.

34. S. Sawada, T. Iio, Y. Hayashi, and S. Takahashi (1992) Fluorescent rotors and their applications to the study of G-F transformation of actin. *Anal. Biochem.* **204**, 110–117.
35. T. Förster and G. Hoffmann (1971) *Zeit. Physikal. Chem.* **75**, 63–76.
36. C. E. Kung and J. K. Reed (1986) Microviscosity measurements of phospholipid bilayers using fluorescent dyes that undergo torsional relaxation. *Biochemistry* **25**, 6114–6121.
37. R. Blumenthal, D. P. Sarkar, S. Durell, D. E. Howard, and S. J. Morris (1996) Dilation of the influenza hemagglutinin fusion pore revealed by the kinetics of individual cell-cell fusion events. *J. Cell Biol.* **135**, 63–71.
38. L. H. Li, M. L. Hensen, Y. L. Zhao, and S. W. Hui (1996) Electrofusion between heterogeneous-sized mammalian cells in a pellet: potential applications in drug delivery and hybridoma formation. *Biophys. J.* **71**, 479–486.
39. R. Ramanathan, M. F. Wilkemeyer, B. Mittal, G. Perides, and M. E. Charness (1996) Alcohol inhibits cell-cell adhesion mediated by human L1. *J. Cell Biol.* **133**, 381–90.
40. B. Ragnarson, L. Bengtsson, and A. Haegerstrand (1992) Labeling with fluorescent carbocyanine dyes of cultured endothelial and smooth muscle cells by growth in dye-containing medium. *Histochemistry* **97**, 329–333.
41. G. W. Gordon, B. Chazotte, X. F. Wang, and B. Herman (1995) Analysis of simulated and experimental fluorescence recovery after photobleaching. Data for two diffusing components. *Biophys. J.* **68**, 766–778.
42. D. E. Wolf, B. K. Scott, and C. F. Millette (1986) The development of regionalized lipid diffusibility in the germ cell plasma membrane during spermatogenesis in the mouse. *J. Cell Biol.* **103**, 1745–1750.
43. R. D. Klausner and D. E. Wolf (1980) Selectivity of fluorescent lipid analogues for lipid domains. *Biochemistry* **23**, 6199–6203.
44. C. H. Spink, M. D. Yeager, and G. W. Feigenson (1990) Partitioning behaviour of indocarbocyanine probes between coexisting gel and fluid phases in model membranes. *Biochim. Biophys. Acta* **30**, 25–33.
45. W. J. Betz and G. S. Bewick (1992) Optical analysis of synaptic vesicle recycling at the frog neuromuscular junction. *Science* **255**, 200.
46. T. A. Vida and S. D. Emr (1995) A new vital stain for visualizing vacuolar membrane dynamics and endocytosis in yeast. *J. Cell Biol.* **128**, 779–792.
47. S. L. Shorte, S. J. Stafford, V. J. Collett, and J. G. Schofield (1995) Simultaneous measurement of Ca^{2+} and secretion-coupled membrane turnover, by single cell fluorescence microscopy. *Cell Calcium* **18**, 440–454.
48. K. L. Hill, N. L. Catlett, and L. S. Weisman (1996) Actin and myosin function in directed vacuole movement during cell division in Saccharomyces cerevisiae. *J. Cell Biol.* **135**, 1535.
49. S. Härtel (2000) *Quantifizierung von Strukturen, Kinetik und Dynamik nekrobiologischer Prozesse mit Hilfe bildverarbeitender konfokaler Fluoreszenzmikroskopie*. Ph.D. Thesis, University of Bremen, Bremen. [The publication is available in *.pdf format from http://elib.suub.uni-bremen.de/dissertations/physic/Haertel_S2000/Haertel_S2000.pdf]
50. P. L. Yeagle (1985) Cholesterol and the cell membrane. *Biochim. Biophys. Acta* **822**, 267–287.
51. K. H. Cheng, L. Ruymgaart, L. I. Liu, and P. Somerharju (1994) Intramolecular excimer kinetics of fluorescent dipyrenyl lipids: 1. DMPC/cholesterol membranes. *Biophys. J.* **67**, 902–913.
52. T. P. W. McMullen and R. N. McElhaney (1994) New aspects of the interaction of cholesterol with DMPC bilayers as revealed by high-sensitive differential scanning calometry. *Biochim. Biophys. Acta* **1234**, 90–98.
53. T. Parasassi, F. Conti, and E. Gratton (1986) Time-resolved fluorescence emission spectra of Laurdan in phospholipid vesicles by multifrequency phase and modulation fluorometry. *Cell. Mol. Biol.* **32**, 103–108.
54. T. Parasassi and E. Gratton (1995) Membrane lipid domains and dynamics as detected by Laurdan fluorescence. *J. Fluoresc.* **51**, 59–69.
55. L. C. Dias, R. Custodio, and F. B. T. Pessine (1999) Theoretical studies of Nile Red by ab initio and semiempirical methods. *Chem. Phys. Lett.* **302**, 505–510.
56. P. Greenspan and S. D. Fowler (1985) Spectrofluorometric studies of the lipid probe nile red. *J. Lipid. Res.* **26**, 781–789.
57. P. Greenspan, E. P. Mayer, and S. D. Fowler (1985) Nile red: a selective fluorescent stain for intracellular lipid droplets. *J. Cell. Biol.* **100**, 965–973.
58. A. K. Dutta, K. Kamada, and K. Ohta (1996) Langmuir-Blodgett films of nile red: a steady-state and time-resolved fluorescence study. *Chem. Phys. Lett.* **258**, 369–375.
59. V. J. P. Srivatsavoy (1999) Enhancement of excited state nonradiative deactivation of Nile Red in γ-cyclodextrin: evidence for multiple inclusion complexes. *J. Luminesc.* **82**, 17–23.
60. P. L. Chong and P. T. Wong (1993) interactions of Laurchan with phosphatidylcholine liposomes: a high pressure FTIR study *Biochim. Biophys. Acta* **1149**, 260–266.
61. P. M. Gocze and D. A. Freeman (1994) Factors underlying the variability of lipid droplet fluorescence in MA-10 Leydig tumor cells. *Cytometry* **17**, 151–158.
62. P. Fromherz and A. Lambacher (1991) Spectra of voltage-sensitive fluorescence of styryl dye in neuron membrane. *Biochim. Biophys. Acta* **30**, 149–156.
63. P. J. Sims, A. S. Waggoner, C. H. Wang, and J. F. Hoffman (1974) Studies on the mechanism by which cyanine dyes measure membrane potential in red blood cells and phosphatidylcholine vesicles. *Biochemistry* **13**, 3315–3330.
64. J. Korlach, P. Schwille, W. W. Webb, and G. W. Feigenson (1999) Characterization of lipid bilayer phases by confocal microscopy and fluorescence correlation spectroscopy. *Proc. Natl. Acad. Sci. USA* **96**, 8461–8466.
65. S. Mukherjee, T. T. Soe, and F. R. Maxfield (1999) Endocytic sorting of lipid analogues differing solely in the chemistry of their hydrophobic tails. *J. Cell. Biol.* **144**, 1271–1284.
66. R. A. Badley, W. G. Martin, and H. Schneider (1973) Dynamic behaviour of fluorescent probes in lipid bilayer model membranes. *Biochemistry* **16**, 268–275.
67. D. Axelrod (1979) Carbocyanine dye orientation in red cell membrane studied by microscopic fluorescence polarization. *Biophys. J.* **26**, 557–574.
68. J. Lee, M. Gustafsson, K. E. Magnusson, and K. Jacobson (1990) The direction of membrane lipid flow in locomoting polymorphonuclear leukocytes. *Science* **9**, 1229–1233.
69. B. S. Packard and D. E. Wolf (1985) Fluorescence lifetimes of carbocyanine lipid analogues in phospholipid bilayers. *Biochemistry* **10**, 5176–5181.
70. D. Gaskova, B. Brodska, P. Herman, J. Vecer, J. Malinsky, K. Sigler, O. Benada, and J. Plasek (1998) Fluorescent probing of membrane potential in walled cells: diS-C3(3) assay in Saccharomyces cerevisiae. *Yeast* **30**, 1189–1197.
71. S. D. Fowler, W. J. Brown, J. Warfel, and P. Greenspan (1987) Use of nile red for the rapid in situ quantitation of lipids on thin-layer chromatograms. *J. Lipid. Res.* **28**, 1225–1232.